

# Observations of trace gases and aerosols over the Indian Ocean during the monsoon transition period

T K MANDAL<sup>1</sup>, ATEEF KHAN<sup>1</sup>, Y NAZEER AHAMMED<sup>1</sup>, R S TANWAR<sup>1</sup>, R S PARMAR<sup>1</sup>, K S ZALPURI<sup>1</sup>, PRABHAT K GUPTA<sup>1</sup>, S L JAIN<sup>1</sup>, RISAL SINGH<sup>1</sup>, A P MITRA<sup>1</sup>, S C GARG<sup>1</sup>, A SURYANARAYANA<sup>2</sup>, V S N MURTY<sup>2</sup>, M DILEEP KUMAR<sup>2</sup> and ANDREW J SHEPHERD<sup>3</sup>

<sup>1</sup>National Physical Laboratory, New Delhi 110 012, India.

<sup>2</sup>National Institute of Oceanography, Dona Paula, Goa 403 004, India.

<sup>3</sup>National Ocean and Atmospheric Administration/Pacific Marine Environmental Laboratory, USA.

Characteristics of trace gases (O<sub>3</sub>, CO, CO<sub>2</sub>, CH<sub>4</sub> and N<sub>2</sub>O) and aerosols (particle size of 2.5 micron) were studied over the Arabian Sea, equatorial Indian Ocean and southwest part of the Bay of Bengal during the monsoon transition period (October–November, 2004). Flow of pollutants is expected from south and southeast Asia during the monsoonal transition period due to the patterns of wind flow which are different from the monsoon period. This is the first detailed report on aerosols and trace gases during the sampled period as the earlier Bay of Bengal Experiment (BOBMEX), Arabian Sea Monsoon Experiment (ARMEX) and Indian Ocean Experiments (INDOEX) were during monsoon seasons. The significant observations during the transition period include: (i) low ozone concentration of the order of 5 ppbv around the equator, (ii) high concentrations of CO<sub>2</sub>, CH<sub>4</sub> and N<sub>2</sub>O and (iii) variations in PM<sub>2.5</sub> of 5–20 µg/m<sup>3</sup>.

## 1. Introduction

Emissions of trace gases and aerosols are increasing due to the fast industrialization in Asia, particularly in China and India. Studies on characteristics of atmospheric tropospheric ozone, CO, CO<sub>2</sub>, CH<sub>4</sub> and N<sub>2</sub>O, and aerosols over the Indian Ocean subcontinent are rather sparse. The earlier measurements of trace gases and aerosols over the Indian Ocean have been carried out mostly during summer (Arabian Sea Monsoon Experiment, ARMEX (Sanjeeva Rao 2005), Bay of Bengal Monsoon Experiment, BOBMEX (Bhat *et al* 2001)) and winter monsoons (Indian Ocean Experiment: INDOEX). Observations during INDOEX (Ramanathan *et al* 2001) show the presence of a large haze layer over the Indian Ocean. Composition of this haze indicates that the continental outflow and long range transport are the major reasons for the pollutants to spread out over a large

area of the Indian Ocean (Lelieveld *et al* 2001). No such detailed results are available during the monsoon transition period over the Arabian Sea and equatorial Indian Ocean. During monsoon periods, the wind is mainly meridional and the zonal wind is weaker over the equatorial Indian Ocean. October and November (withdrawal of monsoon period) are the months of transition when winds over the north Indian Ocean change from southwesterly to northerly and northeasterly bringing aerosols from south and southeast Asia to the equatorial and north Indian Ocean (Kunhikrishnan *et al* 2004).

Ozone acts as a major tropospheric greenhouse gas as well as a precursor of highly reactive hydroxy radical (OH) that drives much of photochemistry in this atmospheric layer (Thompson 1992). The concentration of tropospheric ozone is mainly determined by its *in situ* photochemical production, downward transport from stratosphere,

**Keywords.** Trace gases; aerosols; Indian Ocean; monsoon transition; air pollutants.

quasi-isentropic advection and surface destruction. Halocarbons also play a major role in the destruction of ozone over the ocean. The diurnal cycle of ozone over the ocean is largely governed by advection and destruction where photochemical production is less (de Laat and Lelieveld 2000). Carbon monoxide (CO) is an important trace gas as it can produce or destroy ozone depending on the concentrations of NO–NO<sub>x</sub> (Crutzen 1999). Because of the long lifetime of CO in the boundary layer, it is used as a good tracer of long range atmospheric transport (Dickerson *et al* 2002).

The measurements on surface ozone and CO over the Indian Ocean are very few, including those carried out under the Soviet American Gases and Aerosols Campaign (SAGA-II) and INDOEX campaign (Duli Chand *et al* 2001; Naja *et al* 1999; Lal *et al* 1998; Rhoads *et al* 1997). Recent measurements of atmospheric CH<sub>4</sub> over the Indian Ocean include Rhoads *et al* (1997), as a part of the World Ocean Circulation Experiment (WOCE), and Naja *et al* (1999) and Gupta *et al* (1999) as a part of the INDOEX.

Airborne particles, in particular of the size of 2.5 micron, have the potential to increase both light scattering and light absorption in the atmosphere depending on their nature. Aerosols of this size can traverse long distances (Lelieveld *et al* 2001), and are therefore, treated as tracers of biomass burning. Moreover, these aerosols also have a large impact on health.

The present study is aimed at understanding the distribution and processes regulating trace gases and aerosols during the monsoon transition period. We present here the results obtained in campaign mode observations during the period, October 11 to November 16, 2004 onboard ORV *Sagar Kanya*. To identify the possible flow of pollutants, back trajectory analyses were done using the HYSPLIT4 model.

## 2. Data and instrument details

A UV-based analyzer (Model TECO-49C, Thermo Environmental Inc, Franklin, Massachusetts, USA) was used for measuring surface ozone. The precision of ozone measurement is 1 ppbv with a detection limit of 1 ppbv with a response time of 10 seconds for the entire period of observation. Calibration of the system is done regularly with the help of a built-in ozone generator. The analyzers incorporate corrections due to changes in temperature, pressure in the absorption cell and drift in the intensity of UV lamp. The data presented here are according to local solar time.

Measurements of CO were made using non-dispersive infrared (NDIR) gas filter correlation

analyzer (Model TECO-48CTL, Thermo Environmental Inc, Franklin, Massachusetts, USA). The analyzer operates on the principle of infrared absorption at 4.67  $\mu\text{m}$  vibration–rotation band of CO. The lowest detection limit of the analyzer was 20 ppbv. The analyzer was inter-compared with API CO analyzer (Model API300) and calibrated with NIST traceable standard CO gas of 1 ppm (M/s Praxair, USA) after cruise. The zero check is done every two hours using in-built zero air scrubber. The instrumental (TECO-48CTL) periodic zero drift is corrected before processing the data.

Collection of other trace gases (CH<sub>4</sub>, N<sub>2</sub>O, CO<sub>2</sub>) was done by grab sampling, i.e., flushing the air through glass samplers. The glass samplers were flushed initially for ten minutes. After thorough flushing with ambient air, the air sample was collected above atmospheric pressure (to avoid contamination due to leakage) at the bow of the ship, when it is speeding ahead, and the sampler was locked. While collecting the samples, several precautions have been taken to avoid contamination. These samples were analyzed for CH<sub>4</sub>, CO<sub>2</sub> and N<sub>2</sub>O in the laboratory at NPL, New Delhi, by gas chromatograph (Model Sigma-2000 of Perkin-Elmer, USA) with FID and ECD detectors. A methanizer was used to reduce CO<sub>2</sub> to CH<sub>4</sub> before detection. The NIST traceable standard gases (CH<sub>4</sub> of 5.63 ppm, CO<sub>2</sub> of 500 ppm and N<sub>2</sub>O of 1.05 ppm; M/s Matheson Tri-Gas formerly Matheson Gas Products USA) were used for calibration. Nevertheless, some international comparison of these measurements and calibration would help to sort out observational biases, if any. A total of 43 air samples were collected along the cruise path.

The data on meteorological parameters (temperature, relative humidity, wind speed and wind direction) were obtained as a part of the buoy deployment program of NOAA/PMEL Tropical Atmospheric Ocean (TAO) Project. The details on types of sensors used and their accuracies are listed in table 1 (Freitag *et al* 2001; Lake *et al* 2003).

Samples of aerosols (fine particle size 2.5  $\mu\text{m}$ ) were collected on Whatman GF/A filters using a Fine Particle Sampler (Envirotech Pvt. Ltd., Delhi, APM-411). The suspended particulate matter (SPM) was collected by passing ambient air at a flow rate of 1.0–1.3 m<sup>3</sup>/hour. The difference between the weight of filter paper before and after the sampling yielded the concentration of PM<sub>2.5</sub>. The sampling was done for a period of 24 hours.

To identify the regions of biomass burning, we have used the CO data from MOPITT instrument and also processed the fire data offered by MODIS (Moderate Resolution Imaging

Table 1. Details of the instruments used for the study. It provides the sensor type, manufacturer, resolution, accuracy and range of the observation.

Measurement	Sensor type	Manufacturer: model	Resolution	Range	Accuracy	Comments
Ozone	TECO-49 UV-based	Thermo Electron Corporation, USA	1 ppbv	0–1 ppm	1 ppbv	
Carbon monoxide	TECO-48CTL IR based	Thermo Electron Corporation, USA	10 ppbv	0–10 ppm	20 ppbv	
Air temperature	Pt-100 RTD (resistance recorder)	Rotronic Instrument Corp: MP-100	0.01°C	0–40°C	±0.2°C	Lake <i>et al</i> 2003
Relative humidity	Capacitance	Rotronic Instrument Corp: MP-100	0.4% RH real time 0.02% RH delay mode		±2.7% RH	Lake <i>et al</i> 2003
Wind direction	Propeller	R.M.Young 05103	0.2 m/s		±0.3 m/s	Freitag <i>et al</i> 2001
Wind speed	Vane	R.M.Young 05103	1.4°	0–355	±5–7.8°	Freitag <i>et al</i> 2001

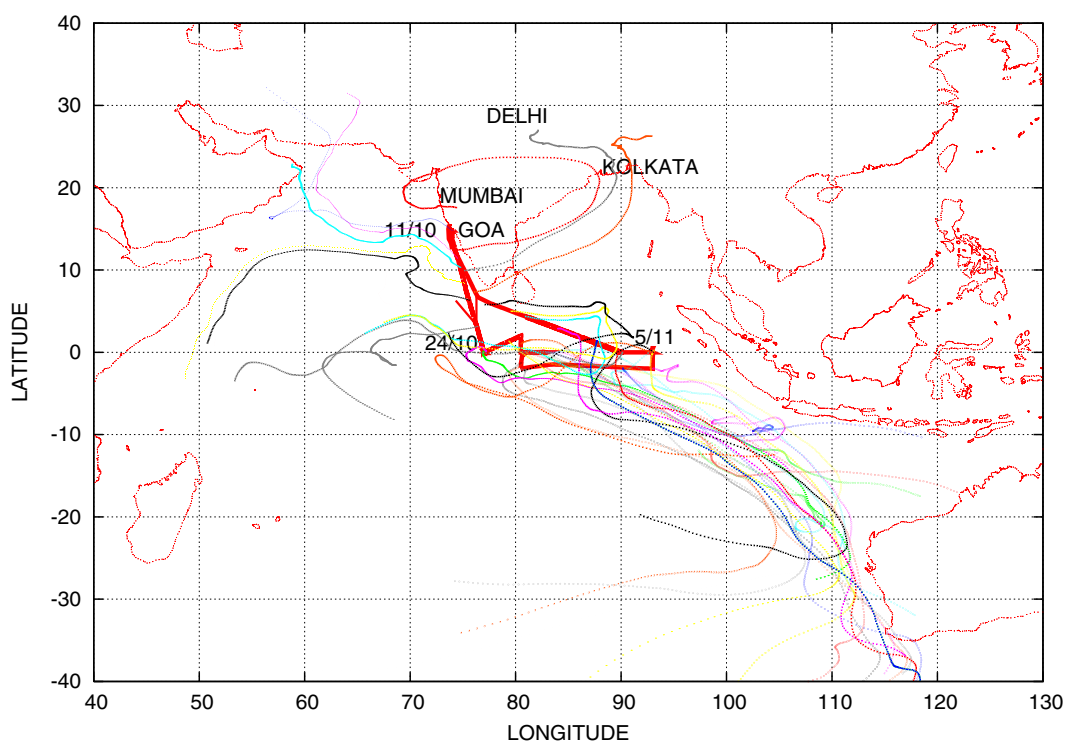


Figure 1. Cruise track and air mass trajectories during this study. The thick line represents the position of ORV *Sagar Kanya*. Thin lines are 10-day back trajectories obtained using HYSPLIT-4 model starting each day at 12:00 hours Local Solar Time at the ship's position.

Spectroradiometer). MOPITT measures the upwelling infrared radiance at wavelengths  $4.7\ \mu\text{m}$  and  $2.3\ \mu\text{m}$  onboard NASA EOS Terra satellite at a height of 705 km (Drummond *et al* 1996). We have used CO mixing ratio at 850 hPa. The methodology of CO retrievals from radiance measurements has been discussed elsewhere in detail (Deter *et al* 2003).

Each of these fire maps shows the locations of the fires detected by MODIS onboard the Terra and Aqua satellites over a 10-day

period (Giglio *et al* 2003). The data of MODIS are based on the measurement of 36 spectral bands between  $0.405$  and  $14.385\ \mu\text{m}$ . These climatological data are available from March 2000 (<http://rapidfire.sci.gsfc.nasa.gov/firemaps/>).

### 3. Ship tracks and meteorology

Figure 1 shows cruise tracks of ORV *Sagar Kanya* (SK 212) with air mass backward trajectories over

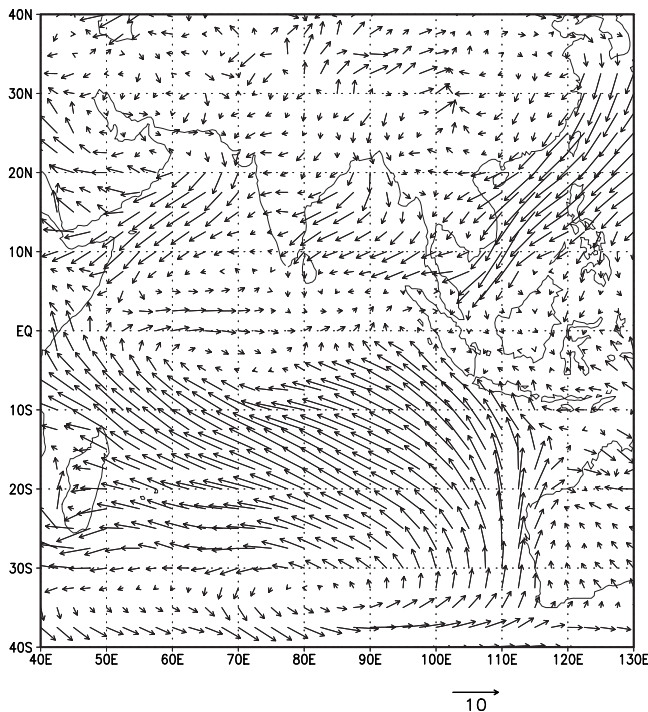


Figure 2. Plot of NCEP/NCAR reanalysis of horizontal wind fields at  $2.5 \times 2.5$  degree resolution averaged over the entire cruise period (October 11 to November 17, 2004) over the region  $40^\circ\text{N}$  to  $40^\circ\text{S}$  and  $40^\circ\text{E}$  to  $130^\circ\text{E}$ . The arrow shown below indicates wind speed of 10 m/s.

the Indian Ocean. Ten days air mass back trajectories were calculated with the HYSPLIT (HYbrid Single-Particle Lagrangian Integrated Trajectory) model (Draxler and Rolph 2003) using FNL as meteorological input data. Meteorological data used were collected onboard *Sagar Kanya*.

Figure 2 presents NCEP/NCAR reanalysis of wind fields at a resolution of  $2.5 \times 2.5$  degree averaged over the entire cruise period (October 11 to November 17, 2004) over the region. Based on the wind flow pattern, the entire cruise period may be divided into three regimes of air parcel movement. During the onward journey, i.e., over the Arabian Sea, wind at surface was mostly northeasterly and upper wind westerly, therefore, air mass originated from the Arabian Sea until ship reached the equator. Once the ship started moving along the equator, the wind was either easterly or southeasterly and hence the air masses originated from south Asia and the Australian subcontinent. On the return journey, flow is north and northeasterly and trajectory calculation shows that air masses originated from the south and southeast Asia. Along the coastal region air mass was mostly from the Indian subcontinent. The measured wind onboard ORV *Sagar Kanya* indicates that the zonal wind ( $u$ ) had dominated over the meridional wind ( $v$ ) up to the equator (figure 3). This is consistent with the NCEP/NCAR reanalysis and general features

of the monsoon transition period. Along the equator, both the meridional wind and zonal wind are very low as observed in the NCEP reanalysis. It may also be pointed that most of the cruise period experienced rainfall.

## 4. Results and discussion

### 4.1 Variation of ozone and its relationship with carbon monoxide

The daily averaged concentrations of ozone, carbon monoxide and relative humidity measured along the cruise path is shown in figure 4. It may be seen that near the coast the ozone concentration was around 16 ppbv and decreased sharply to 7 ppbv and increased to 10 ppbv on October 16, 2004 and then the concentration varied around 10 ppbv. From November 13 ozone concentration showed an increase up to 20 ppbv. Ozone concentration at Bukit Koto ( $0.2^\circ\text{S}$ ,  $100.31^\circ\text{E}$ ), an east Asian station, shows concentration of the order of 10–20 ppbv. Our result is consistent with the observation of Stehr *et al* (2002), whereas, Naja *et al* (1999) and Duli Chand *et al* (2001) reported ozone concentration as high as 50–100 ppbv near the coast during INDOEX. Johnson *et al* (1990) and Duli Chand *et al* (2001) have also found very low ozone of 4 ppbv near the equator. In addition, Naja *et al* (1999) observed a latitudinal gradient of 1.5 ppbv/lat., which is not found in the present study. Results obtained during INDOEX (Lal *et al* 1998; Stehr *et al* 2002; Lelieveld *et al* 2001; Rhoads *et al* 1997) suggested that the region over the northern Indian Ocean is heavily polluted with aerosols and volatile organic carbon (VOC). The low value of ozone could be due to the presence of low  $\text{NO}_x$  concentration over the Indian Ocean (Lal *et al* 1998). The role of prevailing dynamics appears important for sustaining the gradients in trace constituents.

During the onward journey the concentration of CO was 220 ppbv which decreased to 100 ppbv near the equator and then remained between 100 and 150 ppbv. However, on the return journey, CO reached up to 280 ppbv near the coast (figure 4). Naja *et al* (1999) have observed CO concentrations to be between 200 and 350 ppbv in the region from equator to  $15^\circ\text{N}$ . Duli Chand *et al* (2001) observed a similar feature during the final phase of the INDOEX. Stehr *et al* (2002) have found the CO concentration up to a maximum of 200 ppbv in the Arabian Sea and 150 ppbv in the Bay of Bengal. Changes in relative humidity (figure 4) suggest that continental outflow from the Indian subcontinent resulted in the high values of CO near the coastal region. During the observational period,

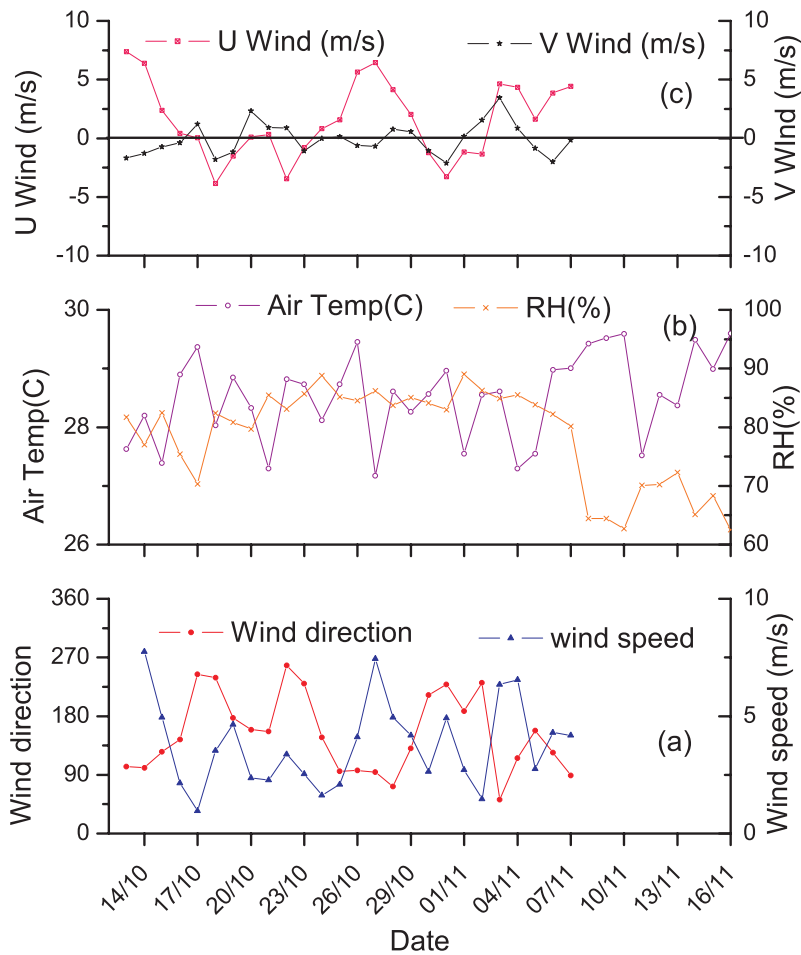


Figure 3. Variations in meteorological parameters observed during cruise period. (a) wind speed (solid triangle) and wind direction (solid circle), (b) relative humidity (%) (cross) and air temperature (open circle) and (c) zonal wind (U) (crossed square) and meridional wind (V) (star).

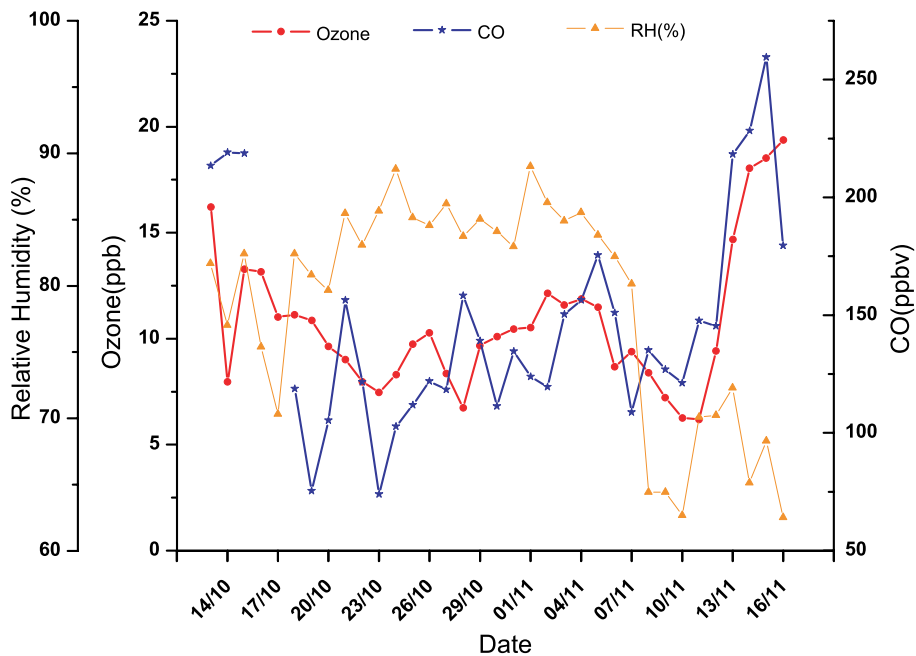
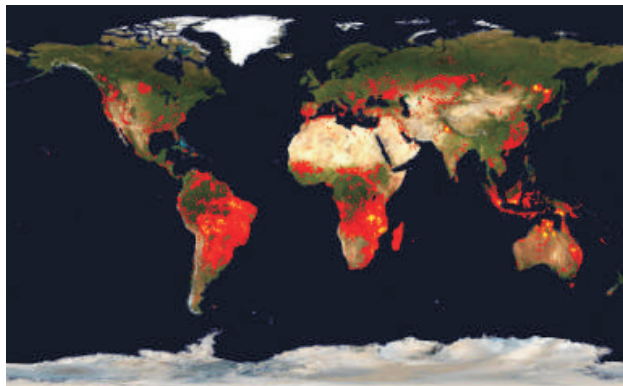
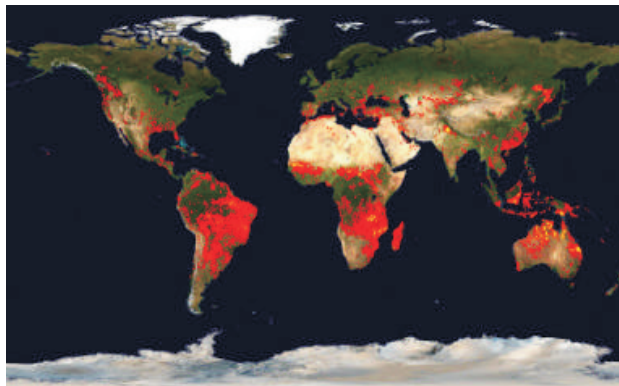


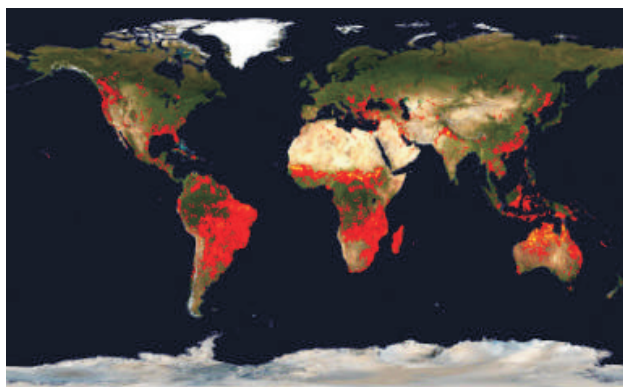
Figure 4. Variations in ozone (solid circle), CO (star) and relative humidity (solid triangle) observed during the cruise. Onward journey of the ship from October 11, 2004 to October 24, 2004, along the equator from October 24, 2004 to November 5, 2004 and return leg from November 5, 2004 to November 17, 2004.



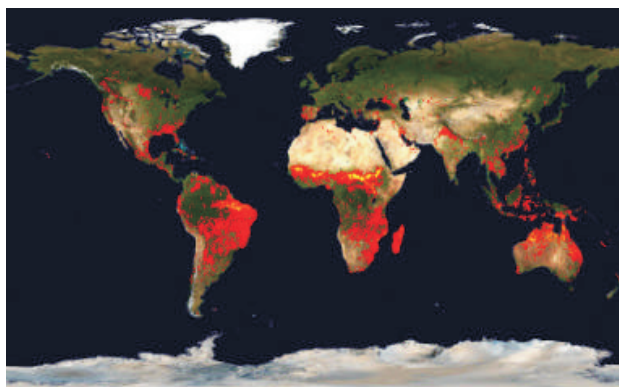
DOY 281–290



DOY 291–300



DOY 301–310



DOY 311–320

Figure 5. Global fire maps averaged over 10 days obtained from processed MODIS data. Fire maps are created at MODIS Rapid Response System at NASA/GSFC. Each of these fire maps shows the locations of fires detected by MODIS onboard the Terra and Aqua satellites. Each coloured dot indicates a location where MODIS detected at least one fire during the compositing period. Colour ranges from red where the fire count is low to yellow where the number of fires is large. The compositing periods are identified by their start and end dates (julian day).

moderate biomass burning events occurred in south and southeast Asia as shown by MODIS data (figure 5). MOPITT data at 850 hPa also shows the presence of high CO concentration ( $< 250$  ppbv) over the same region (figure 6). Backward trajectories show that air masses have mainly originated from south and southeast Asia regions (figure 1). Convection and lightning are very active over Indonesia during the monsoon transition periods, especially during September (Kita *et al* 2003). Nevertheless there is a large interannual variability with enhanced biomass burning during dry El-Niño periods (e.g., September–October, 1997). Dickerson *et al* (2002) have also related high concentration of CO observed over the Indian Ocean to continental outflow from India (emission of CO, 67 Tg/yr) and southeast Asia (emission of CO, 87 Tg/yr).

Figure 7 depicts the diurnal cycle of ozone, CO and relative humidity averaged over the observational period. Although ozone does not

show much diurnal variation (8–12 ppbv CO shows significant changes (120–160 ppbv)), it is to be noted that the time of maximum may not be true as it has been averaged over the region from  $92^{\circ}\text{E}$  to  $72^{\circ}\text{E}$ . Ozone and relative humidity are strongly negatively correlated with CO, particularly during daytime. CO normally acts as a precursor of ozone but about 70% of OH is expected to react with CO (Wanye 1991). Parrish *et al* (1998) observed a positive correlation between ozone and CO while Derwent *et al* (1994) found a negative correlation. Since CO has a lifetime of the order of a month, diurnal variation of CO could be modulated by its long range transport from south and southeast Asia.

#### 4.2 Relationship between PM<sub>2.5</sub> and meteorological parameters

Figure 8 shows the variations in aerosol particle size of  $2.5\ \mu\text{m}$ , relative humidity, wind speeds

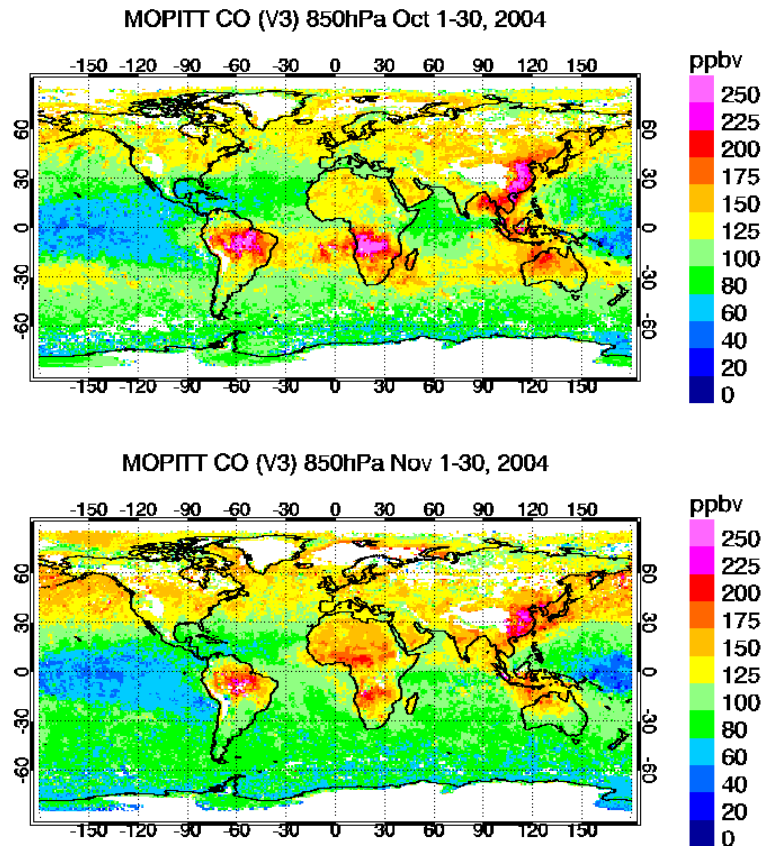


Figure 6. Plot of geographical distribution of carbon monoxide data at 850 hPa obtained through MOPITT satellite. The colour scale on the right side gives the concentration ranges of carbon monoxide. Upper panel shows the averaged CO distribution for the month of October 2004 and the lower panel for the month of November 2004.

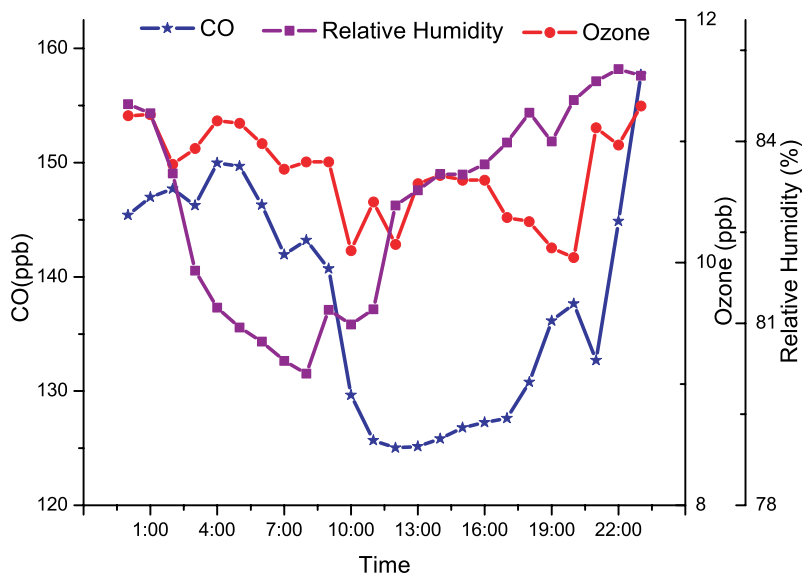


Figure 7. The diurnal cycle of ozone (solid circle), CO (star) and relative humidity (%) (solid square) averaged over the entire cruise period.

observed along the cruise path. The wind speed is positively correlated to aerosol particle size of  $2.5 \mu\text{m}$ . The variation of these particles was within  $5\text{--}20 \mu\text{g}/\text{m}^3$  except near the equator, where its

concentration reached  $37 \mu\text{g}/\text{m}^3$  when wind speed was quite high. Large amounts of sea spray because of high wind ( $7.4 \text{ m/s}$ ) might have been collected on the filter paper. Moreover, the highest value

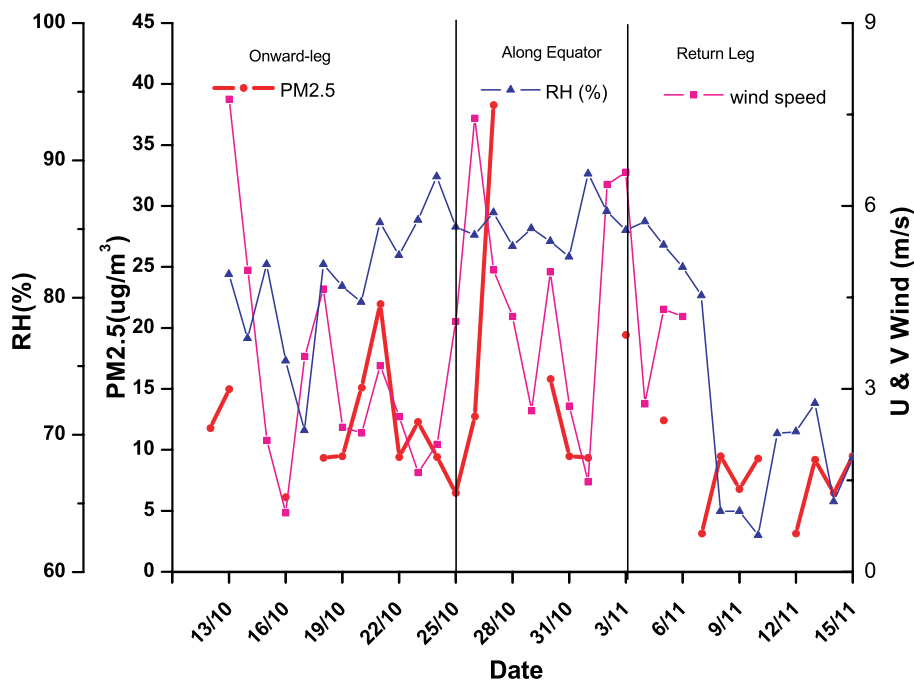


Figure 8. Daily variations of aerosol particle (PM<sub>2.5</sub>) (solid circle), relative humidity (%) (solid triangle) and wind speed (solid square) size measured along the cruise path. The periods of onward journey along the equator and return leg are the same as detailed in figure 4.

of PM<sub>2.5</sub> on October 26–27 could be attributed to long range transport, as air mass back trajectory shows that it had originated from the area of biomass burning (figure 1). During the return leg, even near the coast, the concentration of PM<sub>2.5</sub> dropped to 10  $\mu\text{g}/\text{m}^3$ . It is surprising to note that relative humidity too has come down from 80% to 60%. Relative humidity did not show any variation during the onward journey and along the equator. Chemical composition of these samples may offer better explanation of variation of aerosol concentration. Krishnamurthi *et al* (1998) had also observed fine particle concentration of the order of 15.8  $\mu\text{g}/\text{m}^3$  in the regional plume, which might have been advected to the Indian Ocean during the northeast monsoon. Choudhary *et al* (2001) have shown that the PM<sub>2.5</sub> at Kashidoo Climate Observatory (KCO) varied in the range 15–30  $\mu\text{g}/\text{m}^3$  during winter monsoon time. They have also shown that the sulfate and carbonaceous aerosols are the largest contributors to these fine particles. Ramachandran (2005) has reported background PM<sub>2.5</sub> mass concentration of the order 36 and 25  $\mu\text{g}/\text{m}^3$  over the Arabian Sea and tropical Indian Ocean using the data collected in the northeast winter monsoon seasons of 1996 and 2000, respectively.

#### 4.3 Variation of GHGs

The distributions of CH<sub>4</sub>, CO<sub>2</sub>, N<sub>2</sub>O at surface along the cruise path are shown in figure 9.

Table 2 also gives a comparison between the results obtained in the present and the earlier studies. On an average, the results obtained during the present cruise are higher than earlier reported. The role of contamination in the air samples during the sampling is ruled out as higher values in CH<sub>4</sub>, CO<sub>2</sub>, N<sub>2</sub>O are not observed simultaneously.

The observed concentration of methane is higher than that earlier reported in the northern hemisphere (1.8 ppmv) (Muhle *et al* 2002). The average concentration of methane ranged from 1.69 to 2.7 ppmv. This value is higher than the observed concentration during INDOEX (Naja *et al* 1999; Duli Chand *et al* 2001; Gupta *et al* 1999 and Muhle *et al* 2002). However, Lal *et al* (2006) found high concentrations of CH<sub>4</sub> in the Bay of Bengal to the order of 2.1 ppmv during the early spring of 2001. Near the coast, CH<sub>4</sub> was observed to be  $\sim 2.0$  ppmv, which increased to 2.86 ppmv at the equator with a latitudinal gradient  $-0.06$  ppmv/lat. Naja *et al* (1999) observed that the average gradient of methane concentrations is around 0.0006 ppmv/lat during the pre-INDOEX cruise of 1997 and 1998, whereas, the average gradient during 1999 was found to be 0.0003 ppmv/lat. (Duli Chand *et al* 2001). Although, ocean is normally considered to be a minor source of global tropospheric CH<sub>4</sub>, extensive measurements made by several scientists in the Arabian Sea and coastal India (Lal *et al* 1996; Patra *et al* 1998; Bange *et al* 1998; Jayakumar *et al* 2001) revealed strong



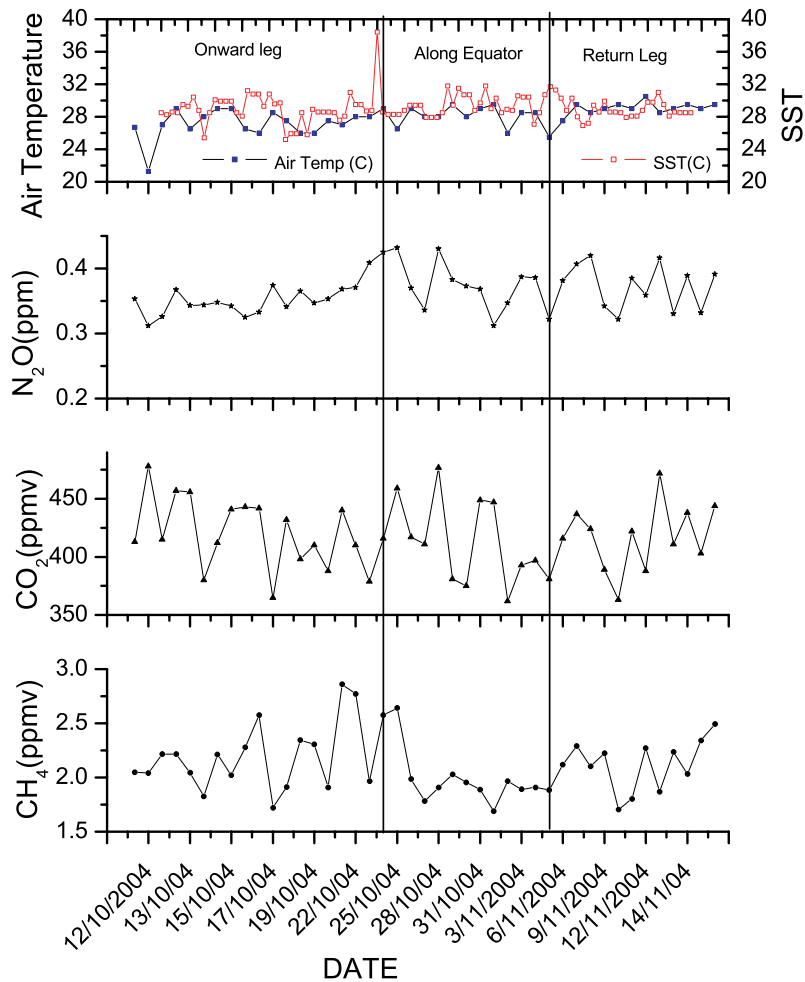


Figure 9. Variations of  $\text{CH}_4$  (solid circle),  $\text{CO}_2$  (solid triangle),  $\text{N}_2\text{O}$  (star) and air temperature (solid square) and SST (open square) observed during the cruise. The periods of onward journey along the equator and return leg are the same as detailed in figure 4.

spatial, seasonal and interannual variability of  $\text{CH}_4$ .

The concentrations of  $\text{CO}_2$  along the cruise were found to be in the range 362–477 ppmv, which is also higher than observed values during INDOEX (Gupta *et al* 1999; Muhle *et al* 2002). High variation of  $\text{CO}_2$  concentration of the order of 100 ppmv within short time scale is normally unexpected, but, no observations are available to compare this result. It may be noted that such variation has only been reported by Mukhopadhyay *et al* (2002), where, they showed  $\text{CO}_2$  concentration of 324.3 to 528.7 ppmv in the Sunderban area, NE coast of Bay of Bengal.  $\text{CO}_2$  concentration reached minimum value 365 ppmv at the equator with a latitudinal gradient of 1 ppmv/lat. but increased again to 477 ppmv. The positive latitudinal gradient observed during onward and return journeys is consistent with the results obtained during pre-INDOEX and final phase of INDOEX by Muhle *et al* (2002) and Gupta *et al* (1999).

JGOFS studies concluded that the Arabian Sea serves as a source of  $\text{CO}_2$  for the atmosphere at almost all places and during all seasons with large variability, whereas, the observations in the Bay of Bengal and the Andaman Sea show that it is a weak sink ( $\sim 20 \text{ Tg C y}^{-1}$ ) for atmospheric  $\text{CO}_2$  (Kumar *et al* 1996; Sarma *et al* 2000; Naqvi *et al* 2005). The 10-day backward trajectories over the Arabian Sea (figure 1) show that the origin of air parcel is oceanic, whereas, the air mass originated from south and southeast Asia, area of biomass burning during the equator and return leg (figures 5 and 6). At this moment, it is difficult to say definitely, with the present limited atmospheric observations that this high  $\text{CO}_2$  concentrations over Arabian Sea are of oceanic origin because of its large lifetime. Sarma *et al* (2000) have argued that bacteria found in seawater are more abundant during intermonsoon period that are not entirely supported by primary production and hence the resultant higher bacterial respiration may raise  $p\text{CO}_2$  levels in the ocean. The Sea Surface Temperature (SST)

Table 2. Comparison of concentration of CH<sub>4</sub>, CO<sub>2</sub> and N<sub>2</sub>O obtained in different studies over Arabian Sea, North Indian Ocean and Bay of Bengal. We have divided the results in the Arabian Sea (onward journey), along the equator (north Indian Ocean) and return journey (partly Bay of Bengal).

CH <sub>4</sub> (ppmv)	Onward journey (Arabian Ocean)		Along the equator (Indian Ocean)		Onward journey (partly Bay of Bengal)			References	
	CO <sub>2</sub> (ppmv)	N <sub>2</sub> O (ppbv)	CH <sub>4</sub> (ppmv)	CO <sub>2</sub> (ppmv)	N <sub>2</sub> O (ppbv)	CH <sub>4</sub> (ppmv)	CO <sub>2</sub> (ppmv)		N <sub>2</sub> O
2.20 ± 0.31 (21)	419.7 ± 29.9 (21)	355.0 ± 27.5 (21)	1.96 ± 0.23 (10)	412.4 ± 37.4 (10)	370.5 ± 37.5 (10)	2.09 ± 0.23 (14)	413.2 ± 29.0 (14)	370.1 ± 35.0 (14)	Present study
1.78	367	315	169.5 ± 7.5	361.2 ± 0.9	312.8 ± 0.3	1.77	367.5	314.4	Muhle et al 2002
2.02	370	320							Gupta et al 1999
1.8			1.6						Naja et al 1999
1.75 ± 0.08			1.65 ± 0.08						Duli Chand et al 2001

Bracket indicates the number of samples used for averaging.

is found to vary from 28° to 32°C (figure 9) and is mostly higher than the air temperature, which varied within 24–28°C. The higher temperature gradient might have facilitated release of CO<sub>2</sub> and N<sub>2</sub>O to the atmosphere.

The concentration of N<sub>2</sub>O near the coast, as depicted in figure 9, was 312 ppbv but reached a maximum of 432 ppbv at the equator with a latitudinal gradient of 2 ppbv/lat. N<sub>2</sub>O concentration then has decreased sharply to 312 ppbv again after the ship entered southern hemisphere. N<sub>2</sub>O concentration does not change substantially along the equator and in the return leg. Surprisingly, the maximum concentration of N<sub>2</sub>O matches with position of maximum concentration of CO<sub>2</sub>. Gupta et al (1999) have not observed any latitudinal gradient in their study during the three pre-INDOEX cruises. With the present data it is difficult to suggest that this high concentration of nitrous oxide is due to upwelling of oceanic water. JGOFS Arabian Sea data show that sea-to-air fluxes of N<sub>2</sub>O over the Arabian Sea are higher particularly in the south Indian coastal region with strong temporal variability (Lal and Patra 1998; Naqvi et al 1998; Patra et al 1999). Total estimates of N<sub>2</sub>O fluxes from the Arabian Sea to the atmosphere ranges between 0.16 and 1.5 Tg N<sub>2</sub>O y<sup>-1</sup>. Naqvi et al (2000) suggested that anomalous concentration of N<sub>2</sub>O in the Arabian Sea could be driven by anthropogenic origin. However, from the present study, we cannot conclude that high concentration of atmospheric N<sub>2</sub>O is of oceanic origin.

## 5. Summary and conclusion

Characteristics of atmospheric surface ozone, CO, CH<sub>4</sub>, N<sub>2</sub>O, CO<sub>2</sub> and aerosol (fine particles) were studied over the Bay of Bengal, the Arabian Sea and the equatorial Indian Ocean during the monsoon transition period, i.e., October–November, 2004.

The following features were found during the campaign:

- The wind flow patterns during monsoon transition period are different from that of monsoons as found from NCEP/NACR reanalysis and onboard measured meteorological parameters. The 10-day backward trajectories suggest that origin of air parcel found over the Arabian Sea is mostly over the ocean, whereas those above the equator and during the return journey are from south or southeast Asia.
- Surface ozone concentration is maximum near coastal region and minimum near equator. No substantial meridional changes are observed in ozone concentrations.

- Carbon monoxide concentration shows similar feature with maximum value near the coast and lowest value near the equator. The observed trend is consistent with the earlier reported results. The role of long range transport from south Asia and southeast Asia, which are regions of biomass burning as seen in MOPITT and MODIS data, is examined.
- The study region is important in terms of sea-to-air exchange of biogenic gases. No atmospheric observation of CH<sub>4</sub>, CO<sub>2</sub> and N<sub>2</sub>O is available during monsoon transition period; therefore, comparative study is not possible at this stage. Large variations of CH<sub>4</sub>, CO<sub>2</sub> and N<sub>2</sub>O concentration over short time scale are however unexpected.
- During onward journey from 15°N to equator, CH<sub>4</sub> and N<sub>2</sub>O show prominent negative gradients, and CO<sub>2</sub> shows positive gradient, whereas, on the return leg CH<sub>4</sub> and CO<sub>2</sub> show positive latitudinal gradients, but N<sub>2</sub>O concentration does not show such trend. Since the Arabian Sea is normally known as a region of biogenic gases emitter, the enhanced concentration of atmospheric CH<sub>4</sub> and N<sub>2</sub>O over Arabian Sea might be due to emission from ocean. The enhanced values over the Bay of Bengal and the equator appear to be linked to biomass burning over east Asia and south east Asia.
- The mass concentration of PM<sub>2.5</sub> varied within 5–20 μg/m<sup>3</sup> except near the equator, where the value reached 37 μg/m<sup>3</sup>. Relative humidity and wind speed are strongly correlated with high concentration of PM<sub>2.5</sub>. Chemical analysis of these samples may give more insight into reasons that caused high concentrations.

### Acknowledgements

Authors are grateful to the Director, National Physical Laboratory, New Delhi for his support. Authors are thankful to CSIR for funding this program under CSIR-Network Activity. Authors acknowledge the TAO Project Office, National Oceanic and Atmospheric Administration, Pacific Marine Environmental Laboratory, USA. The National Institute of Oceanography, Goa is thankfully acknowledged for providing the opportunity to participate in the Buoy Deployment cruise, SST data and logistic support while staying at Goa. The authors also acknowledge the NOAA Air Resources Laboratory (ARL) for permitting the use of their HYSPLIT transport and dispersion model and/or READY website (<http://www.arl.noaa.gov/ready.html>) results used in this publication. We further acknowledge the NOAA-CIRES Climate Diagnostics Center for

the reanalysis data provided at their website at <http://www.cdc.noaa.gov/>. This is NIO contribution no. 4143.

### References

- Bange H W, Ramesh R, Rapsomanikis S and Andreae M O 1998 Methane in surface waters of the Arabian Sea; *Geophys. Res. Lett.* **25** 3547–3550.
- Bhat J S *et al* 2001 BOBMEX: The Bay-of-Bengal Monsoon Experiment, *Bull. Amer. Meteor. Soc.* **82** 2217–2243.
- Choudhary Z, Huges L S, Salmon L G and Cass G R 2001 Atmospheric particle size and composition measurements to support light extinction calculations over the Indian Ocean; *J. Geophys. Res.* **106(D22)** 28,597–28,605.
- Crutzen P J, Lawrence M G and Poschl U 1999 On the background photochemistry of tropospheric ozone; *Tellus Ser A* **51** 123–146.
- Dickerson R R, Andreae M O, Campos T, Mayol-Bracero O L, Neusuess C and Streets D G 2002 Analysis of black carbon and carbon monoxide observed over the Indian Ocean: Implications for emissions and photochemistry; *J. Geophys. Res.* **107(D19)** 8017, doi:10.1029/2001JD000501.
- de Laat A T J and Lelieveld J 2000 Diurnal ozone cycle in the tropical and subtropical marine boundary layer; *J. Geophys. Res.* **105(D9)** 11,547–11,559.
- Derwent R G, Simmonds P G and Collins W J 1994 O<sub>3</sub> and CO measurements at a remote maritime location, Mace Head, Ireland, from 1990 to 1992; *Atmos. Environ.* **28(16)** 2623–2637.
- Deter M N *et al* 2003 Operational carbon monoxide retrieval algorithm and selected results for the MOPITT instruments; *J. Geophys. Res.* **106(D14)** 4399.
- Draxler R R and Rolph G D 2003 HYSPLIT (Hybrid Single-Particle Lagrangian Integrated Trajectory) Model access via NOAA ARL READY Website (<http://www.arl.noaa.gov/ready/hysplit4.html>). NOAA Air Resources Laboratory, Silver Spring, MD.
- Drummond, James R and Mand G S 1996 The measurements of pollution in the troposphere (MOPITT) Instrument: Overall performance and Calibration Requirements, *Journal of Atmospheric and Oceanic Technology* **13** 314.
- Duli Chand, Modh K S, Naja M, Venkataramani S and Shyam Lal 2001 Latitudinal trends in O<sub>3</sub>, CO, CH<sub>4</sub>, SF<sub>6</sub>, over the Indian Ocean during the INDOEX IFF-1999 ship cruise; *Curr. Sci.* **80** (supplement) 100–104.
- Freitag H P, O'Haleck M, Thomas G C and McPhaden M J 2001 Calibration procedures and instrumental accuracies for ATLAS wind measurements, NOAA Tech Memo. OAR PMEL-119, NOAA/Pacific Marine Environmental Laboratory, Seattle, Washington, 20 pp.
- Giglio L, Desclotres J, Justice C O and Kaufman Y J 2003 An enhanced contextual fire detection algorithm for MODIS; *Remote Sensing of Environment* **87** 273–282.
- Gupta, Prabhat K, Sharma C, Koul S, Parashar D C, Mandal T K and Mitra A P 1999 Study of trace gas species including greenhouse gases over the Indian Ocean during INDOEX pre-campaign cruises of 1996, 1997, and 1998 on Sagar Kanya, *Curr. Sci.* **76(7)** 944–946.
- Jayakumar D A, Naqvi S W A, Narvekar P V and Geroge M D 2001 Methane in coastal and offshore waters of the Arabian Sea, *Marine Chemistry* **74** 1–13.
- Johnson J E, Gammon R H, Larson J, Bates T S, Oltmans S J and Farmer C 1990 Ozone in the marine

- boundary layer over the Pacific and Indian Ocean: Latitudinal gradients and diurnal cycles; *J. Geophys. Res.* **95(D8)** 11,847–11,856.
- Kita K *et al* 2003 Photochemical production of ozone in the upper troposphere in association with cumulus convection over Indonesia; *J. Geophys. Res.* **108(D3)** 8400, doi:10.1029/2001JD000844.
- Krishnamurthy K, Satheesh S K and Krishnamurthy B V 1998 Characteristics of special optical depths and size distribution of aerosols over tropical oceanic region; *J. Atmospheric and Solar Terrestrial Phys.* **60** 981–992.
- Kumar M D, Naqvi S W A, George M D and Jayakumar D A 1996 A sink for atmospheric carbon dioxide in the northern Bay of Bengal; *J. Geophys. Res.* **101** 18,121–18,125.
- Kunhikrishnan T, Lawrence M G, von Kuhlmann R, Richter A, Ladstatter-Weibenmayer A and Barrows J P 2004 Semiannual NO<sub>2</sub> plumes during the monsoon transition periods over the central Indian Ocean; *Geophys. Res. Lett.* **31** L08110, doi:10.1029/2003GL019269.
- Lake B J, Noor S M, Freitag H P and McPhaden M J 2003 Calibration procedures and instrumental accuracy estimates of ATLAS air temperature and relative humidity measurements; *NOAA Tech Memo*. OAR PMEL-123, NOAA/Pacific Marine Environmental Laboratory, Seattle, WA, 23 pp.
- Lal S, Patra P K, Venkataramani S and Sarin M M 1996 Distribution of nitrous oxide and methane in the Arabian Sea; *Curr. Sci.* **71** 894–899.
- Lal S, Naja M and Jayaraman A 1998 Ozone in the marine boundary layer over the tropical Indian Ocean; *J. Geophys. Res.* **103(D15)** 18,907–18,917.
- Lal S and Patra P K 1998 Variabilities in the fluxes and annual emissions of nitrous oxide from the Arabian Sea; *Global Biogeochem. Cycles* **12** 321–327.
- Lal S, Chand D, Sahu L K, Venkataramani S, Brasseur G and Schultz M G 2006 High levels of ozone and related gases over the Bay of Bengal during winter and early spring of 2001; *Atmos. Environ.* **40** 1633–1644.
- Lelieveld *et al* 2001 The Indian Ocean Experiment: Widespread air pollution from south and southeast Asia; *Science* **291** 1031–1036.
- Mukhopadhyay S K, Biswas H, De T K, Sen B K, Sen S and Jana T K 2002 Impact of Sunderban mangrove biosphere on the carbon dioxide and methane mixing ratios at the NE coast of Bay of Bengal; *Atmos. Environ.* **36(2)** 629–638.
- Muhle J, Zahn A, Brenninkmeijer C A M, Gros V and Crutzen P J 2002 Air mass classification during the INDOEX R/V Ronald Brown cruise using measurements of nonmethane hydrocarbons, CH<sub>4</sub>, CO<sub>2</sub>, CO, <sup>14</sup>CO, and <sup>18</sup>C(CO); *J. Geophys. Res.* **107(D19)** 8021, doi: 10.1029/2001JD000730.
- Naja M, Shyam Lal, Venkataramani S, Modh K S and Duli Chand 1999 Variabilities in O<sub>3</sub>, NO, CO, and CH<sub>4</sub> over the Indian Ocean during winter; *Curr. Sci.* **7(7)** 931–937.
- Naqvi S W A, Yoshinari T, Jayakumar D A, Altabet M A, Narvekar P V, Devol A H *et al* 1998 Budgetary and biogeochemical implications of N<sub>2</sub>O isotope signatures in the Arabian Sea; *Nature* **394** 462–464.
- Naqvi S W A, Jayakumar D A, Narvekar P V, Naik H, Sarma V V S S, D'Souza W *et al* 2000 Increased marine production of N<sub>2</sub>O due to intensifying anoxia on the Indian continental shelf; *Nature* **408** 346–349.
- Naqvi S W A, Bange H W, Gibb S W, Goyet C, Hatton A D and Upstill-Goddard R C 2005 Biochemical ocean-atmosphere transfers in the Arabian Sea; *Progr. Oceanogr.* **65** 116–144.
- Parrish D D, Trainer M, Holloway J S, Yee J E, Warshawsky M S and Fehsenfeld F C 1998 Relationships between ozone and carbon monoxide at surface sites in the North Atlantic Ocean; *J. Geophys. Res.* **103(D11)** 13,357–13,376.
- Patra P K, Lal S, Venkataramani S, Gauns M and Sarma V V S S 1998 Seasonal variability in distribution and fluxes of methane in the Arabian Sea; *J. Geophys. Res.* **103** 1167–1176.
- Patra P K, Lal S, Venkataramani S, de Sousa S N, Sarma V V S S and Sardesai S 1999 Seasonal and spatial variability in N<sub>2</sub>O distribution in the Arabian Sea; *Deep-Sea Res. I* **46** 529–543.
- Ramachandran S 2005 PM<sub>2.5</sub> mass concentration in comparison with aerosol optical depths over the Arabian Sea and Indian Ocean during winter monsoon; *Atmos. Environ.* **39(10)** 1879–1890.
- Ramanathan *et al* 2001 Indian Ocean Experiment: An Integrated analysis of the climate forcing and effects of the great Indo-Asian haze; *J. Geophys. Res.* **106(D22)** 28,371–28,398.
- Rhoads K P, Dickerson R R, Kelley P, Carsey T, Farmer M, Savie D and Prospero J 1997 The comparison of the troposphere over the Indian Ocean during the monsoonal season; *J. Geophys. Res.* **102(15)** 18,981–18,995.
- Sanjeeva Rao P 2005 Arabian Sea monsoon Experiment, An overview, *Mausam* **56(1)** 1–6.
- Sarma V V S S, Dileep Kumar M, Gauns M and Madhupratap M 2000 Seasonal controls on surface pCO<sub>2</sub> in the central and eastern Arabian Sea; *Proc. Indian Acad. Sci. (Earth Planet. Sci.)* **109(4)** 471–479.
- Stehr J W, Ball W P, Dickerson R R, Doddridge B G, Piety C A and Johnson J E 2002 Latitudinal gradients in O<sub>3</sub> and CO during INDOEX 1999; *J. Geophys. Res.* **107(d19)** 8015, doi: 10.1029/2001JD000446.
- Thompson A M 1992 The oxidizing capacity of the Earth's atmosphere: Probable past and future changes; *Science* **256** 1157–1165.
- Wanye R P 1991 *Chemistry of Atmospheric: An Introduction to the Chemistry of the Atmospheres of Earth, the Planet, and their Satellites* (Oxford University Press) 581 pp.